Biomaterials 31 (2010) 2673–2685

Contents lists available at ScienceDirect

Biomaterials

journal homepage: www.elsevier.com/locate/biomaterials

Cationic fluorine-containing amphiphilic graft copolymers as DNA carriers

Sheng-Dong Xiong [a], Ling Li [a], Jiang Jiang [b], Li-Ping Tong [b], Shuilin Wu [a,b], Zu-Shun Xu [a,b,**], Paul K. Chu [b,*]

[a] Ministry-of-Education Key Laboratory for the Green Preparation and Application of Functional Materials, Hubei University, Wuhan 430062, China
[b] Department of Physics & Materials Science, City University of Hong Kong, Tat Chee Aenue, Kowloon, Hong Kong, China

ARTICLE INFO

Article history:
Received 24 November 2009
Accepted 3 December 2009
Available online 19 January 2010

Keywords:
Fluorocarbon
Graft copolymer
Gene vector
Micelle

ABSTRACT

A series of cationic fluorine-containing amphiphilic graft copolymers P(HFMA-St-MOTAC)-g-PEG comprising poly(hexafluorobutyl methacrylate) (PHFMA) poly(methacryl oxyethyl trimethylammonium chloride) (PMOTAC) polystyrene (PSt) backbones and poly(ethylene glycol) (PEG) side chains are synthesized as a type of non-viral gene vector. The copolymers self-assemble into spherical micelles in the aqueous media and turbidity and cytotoxicity measurements show that those micelles have excellent dispersive stability and low cytotoxicity. The interactions between the copolymers and calf-thymus DNA are studied by fluorescence spectroscopy and viscosity. The former discloses electrostatic interaction, hydrophobic interaction, and hydrogen bonding in the copolymer/DNA system, whereas the latter indicates that these graft copolymers can bind DNA via the electrostatic and classical intercalation modes. The DNA-binding capacity determined by the gel retardation assay and UV–visible spectrophotometry shows that the copolymers have good binding capacity to DNA and a high charge density or HFMA content in the copolymers bode well for DNA-binding. Transmission electron microscopy, photon correlation spectroscopy, and zeta potential data reveal that stable colloidal complexes (particles) can form easily between the copolymer micelles and DNA. Our results suggest that the copolymers are a promising non-viral vector in a gene delivery system.

1. Introduction

In recent years, gene therapy has attracted much attention for its pharmaceutical applications in treating chronic diseases, immunodeficiency, genetic disorders and cancer [1–3]. There are two categories of gene delivery vectors: viral and non-viral vectors [4,5]. Viral gene vectors have high transfection efficiency but suffer from many disadvantages such as risks of strong immunogenicity, inflammatory response, recombination, and carcinogenicity [6,7]. Fast progress in clinical gene therapy has significantly motivated the development of safe and efficient non-viral gene delivery systems which may substitute for viral vectors which still possess inherent safety problems [8,9]. Cationic lipids and cationic polymers are one of the most widely used and extensively studied non-viral vectors [10,11]. Compared to cationic lipids, cationic polymers are stable, easy to manipulate, easy to self-assemble with DNA, and more economical [12].

One of the major drawbacks of cationic polymers non-viral vector based gene delivery is the toxicity related to the positive charge of polymers [13] such as polyethylenimine (PEI) [8,12] and trimethyl chitosan (TMC) [14]. In addition, the strong electrostatic interaction between cationic polymer and DNA deters gene dissociation from its carrier inside cells impeding the access of RNA polymerase to DNA. Consequently, the gene expression level is limited and the high charge density may combine membranes and destroy cell metabolism [15]. To circumvent the problems described above, one rational way is to graft hydrophilic or hydrophobic side chains to cationic polymer backbones to form amphiphilic copolymers [11,14]. These amphiphilic copolymers self-assemble into a nanosize and core–shell micelle architecture in selective solvents. Compared to water-soluble polycations, such self-assembled micellar nanoparticles as non-viral vector have several advantages. First of all, they are able to load DNA and hydrophobic anti-cancer drugs simultaneously to offer potential synergistic effect in cancer therapy [16]. Secondly, instead of mixing water-soluble polycations and DNA to form complexes, which may result in the formation of uncontrollable large particles, micellar nanoparticles with positive charge allow nucleic acid loading after nanoparticle formation and have long circulation time in the bloodstream [17]. This is believed to benefit the construction of size-controllable and monodispersed nucleic acid loaded nanoparticles which may display unique advantages *in vivo*. Thirdly, the nanoscaled

* Corresponding author. Tel.: +852 34427724; fax: +852 27889549.
** Corresponding author. Tel.: +86 27 61120608; fax: +86 27 88665610.
E-mail addresses: zushunxu@hubu.edu.cn (Z.-S. Xu), paul.chu@cityu.edu.hk (P.K. Chu).

0142-9612/$ – see front matter © 2009 Elsevier Ltd. All rights reserved.
doi:10.1016/j.biomaterials.2009.12.014

micelles (<200 nm) reduce non-selective uptake by the reticuloendothelial system (RES) and exhibit enhanced permeability and retention effects (EPR effect) at solid tumor tissue sites [18,19]. In addition, this preparation method can be upscaled to address the large quantity required by therapeutic applications. Several cationic graft or block polymers micelles such as poly (methacryl oxyethyl trimethylammonium chloride)-graft-poly-(oxyethylene) (PMOTAC-g-POE) [15], trimethyl chitosan-g-poly(*N*-isopropylacrylamide) (TMC-g-PNIPAAm) [14], poly(L-lysine)-graft-polyethylene glycol (PLL-g-PEG) [20], polyethylenimine -graft-polyethylene glycol (PEI-g-PEG) [21], folate-polyethylenimine-block-poly(ethylene glycol) (FOL-PEI-b-PEG) [12] have been used as non-viral gene vectors. The hydrophobic force is the main one forming the micelles in an aqueous solution. However, because the hydrophobic force resulting from the hydrophobic chains of the amphiphilic copolymers is weak, the stability of the micelles is not adequate in many applications [22]. These unstable micelles are thus not suitable for compressing DNA into small spherical particles [23]. Big particles cannot be easily endocytosed by cells leading to low transfection efficiency for DNA [8]. Therefore, the dispersive stability of micelles is another bottleneck that needs to be circumvented. In this respect, several ways to stabilize the micelles including shell crosslinking of micelles have been investigated [24,25]. However, these approaches may adversely affect the micellar properties leading to low delivery efficiency.

Owing to the unique characteristics of fluoropolymers such as high hydrophobicity, high thermal and mechanical stability, gas-dissolving capacity, high fluidity, low dielectric constants, oil-and water-repellency, and very interesting surface properties [26–28], attention has recently been paid to amphiphilic copolymers with fluorocarbon–hydrocarbon hybrid architectures. Among these characteristics, the most intriguing are the oleo- and hydrophobicity and high fluidity of fluorine-containing polymers. They have been studied from the perspective of biomedical applications, for instance, blood substitutes, gas carriers, bioconversion, extraction, and so forth and cannot be achieved by non-fluorinated copolymers [29–32]. Furthermore, because of the oleo- and hydrophobicity of fluorine-containing amphiphilic copolymers, they have very low critical micelle concentrations (CMC) compared to other amphiphilic copolymers [27]. Hence, they have a strong tendency to self-aggregate into stable, well-organized micelles, and these micelles may have unique advantages in drug delivery because they can transmit both hydrophobic and fluorophilic molecules at the same time to the target sites due to the high fluidity, hydrophobicity, and water- and oil-repellency of fluoropolymers [33,34].

Poly(ethylene glycol) (PEG) is widely used as the hydrophilic side chains in amphiphilic graft copolymers. It is a low cost commercial product that possesses some unique and outstanding properties such as hydrophilicity, biocompatibility, nontoxicity, lack of immunogenicity, metal complexing ability, as well as solubility in water and organic solvents. Recently, PEG has been widely applied in gene delivery systems. The presence of PEG on the surface of gene vectors can enhance biocompatibility, reduce cytotoxicity, and protect DNA from degradation [12,35,36].

There have been few reports on the use of self-assembled cationic fluorine-containing amphiphilic copolymer micelles in DNA delivery. The present study aims at the synthesis of cationic fluorine-containing amphiphilic copolymers P(HFMA-St-MOTAC)-g-PEG with hydrophobic poly(hexafluorobutyl methacrylate) (PHFMA), poly(methacryl oxyethyl trimethylammonium chloride) (PMOTAC), polystyrene backbones and poly(ethylene glycol) (PEG) side chains. Because of the hydrophobic characteristic of the fluorinated segment which induces the micellar core formation and stabilizes the nanoparticles, the amphiphilic graft copolymer has a good and stable self-assembled morphology in aqueous media. Meanwhile, on account of the positively charged MOTAC segment, it serves as a DNA-binding site, and hydrophilic poly(ethylene glycol) (PEG) can also potentially protect the DNA and extend blood circulation in systemic administration. These unique tri-layered cationic fluorine-containing amphiphilic graft copolymer micelles are used as a non-viral gene vector. The dispersive stability of these micelles in aqueous media is evaluated and the *in vitro* cytotoxicity of the resulting copolymers is examined. The physiochemical characteristics of the copolymer/DNA complexes are analyzed by fluorescence, viscosity, agarose gel electrophoresis, UV spectrophotometry, particle size, transmission electron microscopy, and zeta potential measurements.

2. Materials and methods

2.1. Materials

2,2,3,4,4,4-Hexafluorobutyl methacrylate (HFMA) was purchased from Xeogia Fluorine–Silicon Chemical Company (Harbin, China, chemical purity) and distilled under reduced pressure before use. Methoxy poly(ethylene glycol) (MPEG) (average molecular weight of 5000 g/mol) was obtained from Aldrich and purified by vacuum-drying at room temperature for 24 h before use. An aqueous solution (75 wt%) of methacryl oxyethyl trimethylammonium chloride (MOTAC) was purchased from Aldrich and used as received. Tetrahydrofuran (THF) purchased from Shanghai Chemical Reagents Co. (Shanghai, China, chemical purity) serving as the solvent was initially dried over potassium hydroxide at least overnight and then refluxed over sodium wire for 3 days before use. Analytical grade 2,2′-azobisisobutyronitrile (AIBN) was purified by recrystallization in ethanol. Sodium hydride (NaH, Nacalai, Kyoto, Japan) and *p*-Chloromethylstyrene (CMSt) supplied by Acros Organics (>95%, Belgium) were used without further purification.

Dulbecco's modified Eagle medium (DMEM) was purchased from Invitrogen Corp. Fetal bovine serum (FBS) was purchased from Hyclone. MTT was purchased from Sigma (St. Louis, MO, USA). Two different types of DNAs, pEGFP-C1 plasmid (gel retardation assay experiments), and calf-thymus DNA (all other experiments) were used in the study. Calf-thymus DNA was purchased from Sigma (St. Louis, MO, USA). The stock solution of calf-thymus DNA was prepared by dissolving DNA in doubly distilled water at 0–4 °C. Plasmid pEGFPC1 encoding a red-shifted variant of wild-type green fluorescent protein (GFP) was purchased from Clontech, Mountain View, CA, USA. pEGFP-C1 plasmids were amplified in the Luria–Bertani medium at 37 °C overnight at 250 rpm. Then the plasmids were purified by means of EndoFree plasmid purification. The purified plasmid was diluted by tris–EDTA buffer solution and stored at −20 °C. All other reagents and solvents were used as received without further purification. Distilled water was used in all the preparation and characterization processes.

2.2. Synthesis of P(HFMA-St-MOTAC)-g-PEG

2.2.1. Synthesis of SPEG macromonomers

MPEG (10.000 g, 2 mmol) was dissolved in dry THF (100 mL) and NaH (0.072 g, 3 mmol) was added by stirring at 45 °C for 2 h. After CMSt (1.220 g, 8 mmol) was added into the flask, the reaction was conducted at 35 °C for 24 h. The products were precipitated using a large amount of diethyl ether and filtered. They were purified by dissolving in CH_2Cl_2 and filtered to remove any insoluble impurities. Finally, the products were precipitated using cold diethyl ether, filtered, and dried under high vacuum [37,38]. The synthesis route of the SPEG macromonomers is illustrated in Scheme 1. The yield was calculated from the weight of the dry SPEG macromonomers obtained. The composition and content of the terminal vinyl group in SPEG macromonomers was quantified according to the ^{1}H NMR spectrum.

2.2.2. Synthesis of P(HFMA-St-MOTAC)-g-PEG graft copolymer

The graft copolymers were synthesized via conventional free radical polymerization in THF. In a typical reaction, SPEG macromonomer (1.420 g, 0.277 mmol), HFMA (2.400 g, 9.600 mmol), MOTAC (0.180 g, 0.867 mmol), AIBN (0.024 g 0.146 mmol), and THF (20 mL) were added into a 50 mL round bottom flask containing a magnetic stirrer. The flask was then deoxygenated under reduced pressure and backfilled with nitrogen several times. Polymerization was carried out at 75 °C for 20 h. The product was isolated by evaporating the solvent in a rotary evaporator and then the mixture was precipitated in *n*-hexane. After filtration, the precipitate was purified by re-precipitation repeatedly in *n*-hexane. The obtained product was dried under vacuum at 35 °C for 72 h. Polymerization conversion was determined by gravimetric analysis. The product was analyzed by FTIR, ^{1}H NMR, and ^{19}F NMR spectroscopy. The detailed polymerization conditions are listed in Table 1.

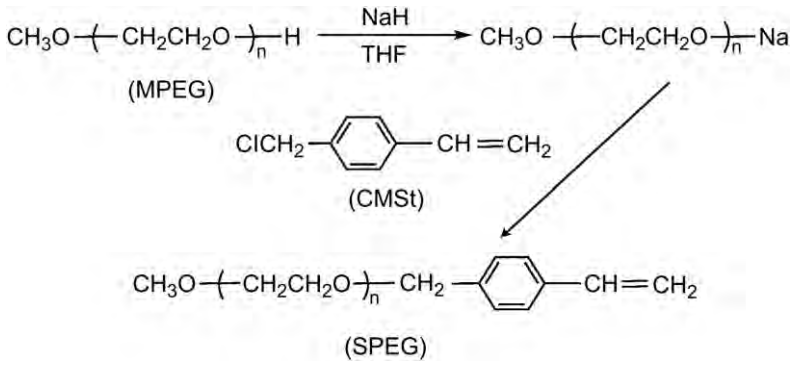

Scheme 1. Synthesis route of SPEG macromonomers.

2.3. Characterization

FTIR spectra of macromonomer and graft copolymer were acquired on the Perkin–Elmer Spectrum one Transform Infrared Spectrometer (Perkin–Elmer, USA). The polymer films were cast onto KBr disks from tetrahydrofuran solutions. The FTIR spectra were recorded from 4000 to 400 cm^{-1}. ^1H NMR and ^{19}F NMR spectra were recorded using a UNITY INVOA-600 MHz spectrometer (Varian, USA) at 20 °C with $CDCl_3$ as the solvent. The content of the terminal vinyl group in the PEG macromonomer was quantified by means of ^1H NMR according to the peak intensity ratio of the $–CH_2–$ protons to $CH_3O–$ proton. The HFMA and MOTAC contents in the graft copolymers were calculated by the ^1H NMR peak intensity ratios of the $–CH_2–$ protons of HFMA, $–N(CH_3)_3Cl$ protons of MOTAC and the $CH_3O–$ proton of the SPEG macromonomer. The molecular weight and molecular weight distribution of SPEG macromonomer and P(HFMA-St-MOTAC)-g-PEG were determined by a Waters 150-C gel permeation chromatograph (GPC) at 30 °C. THF was used as the eluent at a flow rate of 1.0 mL min^{-1}, and polystyrene standards were used for calibration.

2.4. Preparation of graft copolymer solution and copolymer/DNA complexes

The aqueous stock solutions of the copolymers were prepared by dissolving the pure copolymers in distilled water. The solutions were obtained after overnight stirring at room temperature. In some cases, ultrasonic treatment for a few minutes was carried out in addition to stirring in order to obtain clear solutions. The freshly prepared stock solutions were diluted to different concentrations in all other experiments. All the copolymer/DNA complexes were prepared freshly before use. The copolymer solutions were added to the calf-thymus DNA solutions in different volumes, mixed by vortexing for 15 s, and incubated for 10 min before use. Unless otherwise stated, the copolymer/DNA complexes solution did not contain other buffering solutions or reagents. The calf-thymus DNA stock solutions were diluted to a concentration of 3 mg/mL (viscosity studies) or to 90 mg/L (all other experiments).

2.5. Determination of critical micelle concentration (CMC)

The critical micelle concentrations (CMC) for the different copolymers were determined using the fluorescent probe technique. Nile Red was chosen as the hydrophobic dye constituting the micellar payload because its fluorescence is negligible in an aqueous solution, but it is known to increase substantially in a hydrophobic environment found in some membranes or micelles [39]. The samples for spectroscopic analysis were prepared as follows. A Nile red stock solution (2 g/L) was prepared in distilled water and stored until used. The Nile red (3 μL) solution was placed in 5 mL flasks. The polymer solutions of various concentrations were then added into the 5 mL flasks. The obtained solutions were used to obtain the fluorescence spectra at ambient temperature on the RF-540 (Hitachi high-technologies corporation, Tokyo, Japan) spectrofluorimeter at 25 °C. The excitation wavelength was 545 nm. The fluorescence emission spectra were recorded in the wavelength range of 400–750 nm at an angle of 90°. Both the excitation and emission slits were 5 nm.

2.6. In vitro cytotoxicity test

The relative cytotoxicity of P(HFMA-St-MOTAC)-g-PEG graft copolymer was measured by an MTT viability assay against CHO (Chinese Hamster Ovary) cells. The cells were seeded in 96-well plates at 3000 cells/well in 200 μL of the complete medium containing DMEM:F12 (1:1) supplemental medium and 10% fetal bovine serum and incubated at 37 °C in a 5% CO_2 atmosphere for 24 h. The culture medium was the removed and added to the P(HFMA-St-MOTAC)-g-PEG graft copolymer solutions (dose diluted by complete medium) at different concentrations (0–1 g/L). At the end of 24 h of incubation, the medium was removed and 25 μL of the MTT stock solution (5 g/L in PBS) was added to each well to achieve a finial concentration of 1 g/L. The cultures were incubated for another 4 h. The supernatant was removed and 100 μL DMSO was added to dissolve the formazan crystals converted by the catalysis of mitochondrial dehydrogenase from a water-soluble tetrazolium salt. The absorbance of this solution was measured at 570 nm using a Microplate reader. The relative cell viability was calculated by the following equation: relative cell viability (%) = $(OD_{treated}/OD_{control}) \times 100$, where $OD_{control}$ was obtained in the absence of copolymers and $OD_{treated}$ was obtained in the presence of copolymers.

2.7. Fluorescence

The fluorescence properties of a series of graft copolymers in the absence and presence of DNA (without other buffer solutions) were studied on a RF-540 (Hitachi high-technologies corporation, Tokyo, Japan) spectrometer. The fluorescence emission spectra were recorded in the wavelength range 320–520 nm by exciting the P(HFMA-MOTAC)-g-PEG at 300 nm. Both the excitation and emission slits were 5 nm.

2.8. Viscosity measurements

Viscosity measurements were carried out using an Ostwald's capillary viscometer maintained at a constant temperature of 30.0 ± 0.1 °C in a thermostatic bath. Several time readings were obtained at each titration point with a digital stopwatch and an average flow time was calculated. The data were presented as (η/η_0) vs. the binding ratio [40], were η is the viscosity of DNA in the presence of the graft copolymers (without other buffer solutions) and η_0 is the viscosity of DNA alone. The viscosity values were calculated from the observed flow time of DNA containing solution ($t > 100$ s) corrected for the flow time of the buffer alone (t_0), $\eta = t - t_0$.

Table 1
Monomer feed ratios, conversion, and characteristic data of the graft copolymers.

Sample code	SPEG (g)	HFMA (g)	MOTAC (g)	Conversion (%)	Wt.% PFMA (theoretical)	Wt.% MOTAC (theoretical)	Wt.% PFMA (^1H NMR results)[a]	Wt.% MOTAC (^1H NMR results)[a]	$M_n \times 10^5$ (M_w/M_n)[b]	CMC (g/L)[c]
1(PEG-F48M2.1)	1.912	2.000	0.088	97.9	50	2.2	48	2.1	1.62(1.71)	6.51×10^{-2}
2(PEG-F61M2.1)	1.436	2.480	0.084	95.6	62	2.1	61	2.1	1.04(1.86)	1.11×10^{-2}
3(PEG-F67M2.2)	1.112	2.800	0.088	93.6	70	2.2	67	2.2	0.78(1.94)	0.41×10^{-2}
4(PEG-F60M4.5)	1.420	2.400	0.180	95.0	60	4.5	60	4.5	1.02(1.79)	1.09×10^{-2}
5(PEG-F61M6.5)	1.212	2.520	0.268	95.4	63	6.7	61	6.5	0.96(1.99)	1.10×10^{-2}

[a] NMR results.
[b] GPC results.
[c] fluorescence measurements results.

2.9. Gel retardation assay

The DNA condensing ability of P(HFMA-St-MOTAC)-g-PEG was examined by agarose gel electrophoresis. The complexes at different weight ratios were prepared by adding an appropriate volume of P(HFMA-St-MOTAC)-g-PEG solution to 100 ng of pEGFP-C1 (150 ng/μL in 40 mM Tris–HCl buffer solution). The complexes were diluted with 150 mM NaCl solution to 6 μL and then the complexes were incubated at 37 °C for 30 min. Afterwards, the complexes were electrophoresed in the 0.7% (w/v) agarose gel containing GelRed (an ethidium-bromide (EtBr) containing 1%) and with Tris-acetate (TAE) running buffer at 80 V for 100 min. The DNA was visualized with a UV lamp on a Vilber Lourmat imaging system (France).

2.10. UV–visible spectroscopy

The DNA-binding ability of P(HFMA-St-MOTAC)-g-PEG was determined by measuring the intrinsic absorption peaks at 260 nm using a Perkin–Elmer lambda 17 UV–vis spectrophotometer at room temperature. In a typical example, the appropriate volume of DNA solution (90 mg/L) was added to a fixed amount (1 mL) of polymer solution (0.12 g/L). After 24 h of incubation at room temperature, the complexes were centrifuged at 12 000 rpm for 10 min to precipitate the micelles. The amount of unadsorbed DNA was determined using UV–vis spectrophotometer by incubating 50 μL of the supernatant. All the measurements were made in a quartz cuvette (1 cm in width) in the wavelength range of 200–400 nm and the absorption peaks at 260 nm for DNA was used. Deionized water/DNA were used in the comparative experiments.

2.11. Transmission electron microscopy

The morphology of the graft copolymer micelles and the morphology of graft copolymer/DNA complexes were characterized with TEM (Tecnai G20, FEI Corp. USA). The sample was stained with phospho-tungstic acid (pH = 6.5), and a drop of the sample (concentration of graft copolymer solution was above CMC) was placed on a Formvar-coated copper grid which was dried in air. The TEM images were obtained at 25 °C at an electron acceleration voltage of 80 kV.

2.12. Particle size measurement

The average hydrodynamic radius and size distribution of the copolymer micelles and graft copolymer/DNA complexes were measured by photon correlation spectroscopy (PCS) (Autosize Loc-Fc-963, Malvern Instrument). The experiments were performed using the graft copolymer solutions having concentration above CMC. The samples prepared by filtering the solutions through cellulose acetate filters with 0.2 μm pore size were directly poured into a cuvette. The cuvette was then set inside a sample holder. Measurements were made at an angle of 90° with 679 nm wavelength laser light. All the data were averaged from 3 to 5 parallel measurements.

2.13. Stability of copolymer micelles and copolymer/DNA complex particles

The stability of the copolymer micelles in aqueous solutions was evaluated by turbidity measurement and monitoring the time-dependent changes in the micelle size with photon correlation spectroscopy (PCS). The copolymer solutions with the concentrations above CMC were used in this evaluation. The copolymer micelle solutions were incubated at 37 °C for certain durations (1–15 days), followed by turbidity measurement of the suspension at 550 nm. The stability of copolymer/DNA complex particles was examined by monitoring the time-dependent changes in the micelle size (with photon correlation spectroscopy (PCS)) and zeta potentials of these particles.

2.14. Zeta potential measurement

The zeta potentials of the graft copolymer/DNA complexes were measured using Nano-ZS ZEN3600 (Malvern Instruments, Southborough, MA) based on the principle of phase analysis light scattering. The zeta potentials quoted were averages obtained from at least six measurements over duplicate samples.

3. Results and discussion

3.1. Synthesis and characterization of SPEG macromonomer and P(HFMA-St-MOTAC)-g-PEG graft copolymers

Recent development of macromonomer techniques has enabled the preparation of a variety of graft copolymers with a well-defined structure. In this work, we prepare methoxy poly(ethylene glycol) macromonomer (SPEG) with the *p*-vinylbenzyl end group. The synthesis route of the SPEG macromonomer is illustrated in Scheme 1. There is no polymerization reaction during the macromonomer preparation at 35 °C as revealed by the nature of the product as well as ^{1}H NMR and FTIR spectra. The quantitative results are given in Table 2. It is obvious that the P(HFMA-St-MOTAC)-g-PEG graft copolymer can be easily obtained via copolymerization of the SPEG macromonomer, MOTAC, and HFMA using THF as the solvent and AIBN as the initiator. The chemical structure and molecular weight of the graft copolymers and SPEG macromonomer will be discussed in detail later in this paper.

Table 2
Quantitative results of the SPEG macromonomer.

Sample	*Mn*(theoretical)	$M_n(M_w/M_n)$[a]	Amount of vinyl group (%)[b]	Yield (%)
SPEG	5116	5340(1.24)	85	96.8

[a] GPC results.
[b] NMR results.

Fig. 1 shows the FTIR spectra of (A) MPEG, (B) SPEG macromonomer, and (C) P(HFMA-St-MOTAC)-g-PEG. The FTIR spectrum of the MPEG exhibits the characteristic strong absorption of ether linkage at 1120 cm^{-1} and hydroxyl group at 3500 cm^{-1}. Strong absorption by methylene can also be observed at 2800–3000 cm^{-1}. Compared to the spectrum of MPEG, the characteristic strong absorption of the hydroxyl group at 3500 cm^{-1} decreases significantly and the characteristic peak of the double bond at 1640 cm^{-1} is also observed from the SPEG macromonomer. Those at 3000 cm^{-1}, 790 cm^{-1}, 1800–1400 cm^{-1} observed from the SPEG macromonomer (B) are the characteristic absorption peaks of the substituting benzene ring. These modes confirm that the MPEG has been successfully converted into the SPEG macromonomer which contains the double bond and can act as the macromonomer for the synthesis of P(HFMA-St-MOTAC)-g-PEG.

The FTIR spectrum of the P(HFMA-St-MOTAC)-g-PEG copolymer is shown in Fig. 1(C). The characteristic absorption of the double bond at 1640 cm^{-1} disappears, indicating that the monomers have polymerized. The characteristic stretching peak of the C=O group appears at 1700 cm^{-1} because the HFMA and MOTAC contain C=O groups. The absorbance values at 1453 cm^{-1} [–N–$(CH_3)_3$] are characteristic of the MOTAC units. In comparison with the FTIR spectrum of the SPEG macromonomer (B), the FTIR absorption peaks at 1000–1260 cm^{-1} are wider and blunter because of the overlap between the stretching vibration absorption of the C–F

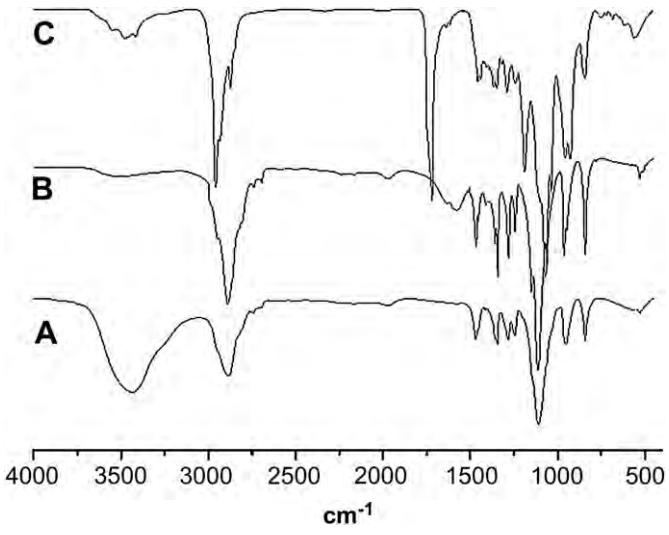

Fig. 1. FTIR spectra of (A) MPEG (B) SPEG, and (C) P(HFMA-St-MOTAC)-g-PEG.

bond at 1100–1260 cm^{-1} and the stretching vibration absorption of the C–O–C bond at 1250 cm^{-1}. This result proves that HFMA, MOTAC and SPEG participate in the polymerization.

The ^1H NMR spectrum of the SPEG macromonomer and peak assignments is presented in Fig. 2(A). The broad peak at 3.65 ppm (b) is assigned to $-CH_2CH_2O-$, the singlet at 3.38 ppm (a) is assigned to CH_3O-, the singlet at 4.58 ppm (c) can be assigned to $-CH_2-$, the peak at 7.4 ppm (d) corresponds to the phenyl protons of the styrene units, and the characteristic peaks at approximately 6.71–5.22 ppm (e,f) are attributed to $-CH{=}CH_2$. The ^1H NMR spectrum clearly demonstrates that the SPEG macromonomer is obtained. The content of the terminal vinyl group in the SPEG macromonomer is quantitatively determined by the peak intensity ratio of the methylene protons 4.58 ppm (c) to the terminal methoxy protons 3.38 ppm (a). The amount of the vinyl group in the macromonomers is calculated to be 85% and the yield of the SPEG macromonomer is 96.8%. The SPEG macromonomer possesses considerably high active functionality and the quantitative results are given in Table 2.

By controlling the experimental protocols, a series of graft copolymers are obtained via conventional free radical polymerization using THF as the solvent and AIBN as the initiator. The ^1H NMR spectrum and assignment of the signals derived from of a typical graft copolymer are shown in Fig. 2(B). In comparison with the ^1H NMR spectrum of the SPEG macromonomer shown in Fig. 2(A), several new peaks from the graft copolymer can be ascribed to the protons of the HFMA and MOTAC segments. For instance, the signals due to terminal methyl group protons are seen at approximately 0.75–1.3 ppm (g) and the signal of methylene protons ($-OCH_2-CF_2-$) at 4.39 ppm (h) is due to the influence of ester group and difluoromethylene ($-CF_2-$). The signal of the characteristic proton of $-N(CH_3)_3Cl$ for the MOTAC part is visible at 3.21 ppm (l). The peaks at 3.66 (b) and 3.3 ppm (a) are attributable to the methylene protons and terminal methoxy protons of PEG. No signals from the protons associated with double bond of unreacted monomer can be detected from this ^1H NMR spectrum. The HFMA and MOTAC contents in the graft copolymers are calculated by the ($-OCH_2-CF_2-$) protons (δ = 4.39 ppm) of HFMA, ($-N(CH_3)_3Cl$) protons (δ = 3.21 ppm) of MOTAC and (CH_3O-) proton (δ = 3.38 ppm) of the SPEG macromonomer. Table 1 summarizes the HFMA and MOTAC contents in each graft copolymers. Here, the abbreviation scheme PEG-F_XM_Z is used, where X represents the HFMA wt% in the graft copolymer and Z represents the MOTAC wt% in the graft copolymer. Hence, for example, PEG-F60M4.5 is a graft copolymer with 60 wt% of HFMA and 4.5 wt% of MOTAC in the backbones.

To better characterize the structure of the graft copolymer, ^{19}F NMR is used to determine the fluorocarbon moiety in the

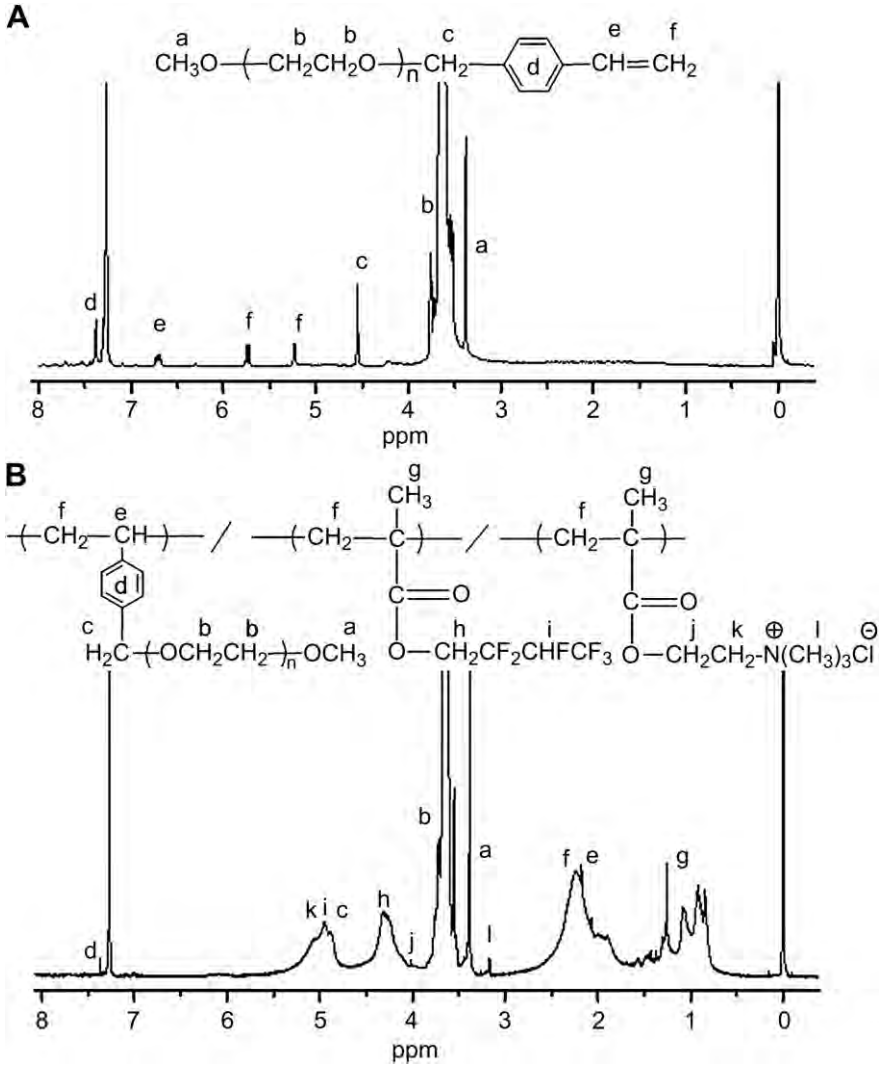

Fig. 2. ^1H NMR spectra of (A) SPEG macromonomer and (B) P(HFMA-St-MOTAC)-g-PEG.

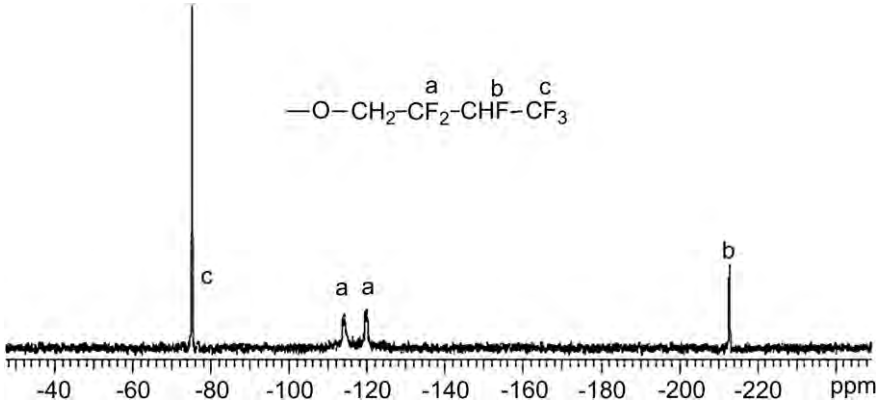

Fig. 3. ^{19}F NMR spectrum of P(HFMA-St-MOTAC)-g-PEG graft copolymer.

copolymer. The ^{19}F NMR spectrum of the graft copolymer depicted in Fig. 3 confirms the presence of three different kinds of fluorine resonances originating from the HFMA side chains. The singlet at −75.2 ppm is assigned to the end –CF_3 group and that at −212.9 ppm to the –CHF_2 group. Because of the influence of the –OCH_2– group, the peak of –OCH_2–CF_2– splits into two peaks at −114.3 ppm and −119.6 ppm. The ^{1}H NMR and ^{19}F NMR results confirm that the graft copolymers have been successfully prepared.

The molecular weight and molecular weight distribution of the SPEG macromonomer and P(HFMA-St-MOTAC)-g-PEG graft copolymers are determined by GPC. Chromatograms recorded from the initial SPEG macromonomer and graft copolymers are shown in Fig. 4. These chromatograms indicate a unimodal molecular weight distribution in both cases and an increase in the molecular weight as result of graft copolymerization. The molecular weight of the SPEG macromonomer determined by GPC (5340 g/mol) is found to be quite close to that predicted theoretically (5116 g/mol). The molecular weight and distribution of the SPEG macromonomer and graft copolymers measured by the GPC instrument are displayed in Tables 1 and 2. The results of GPC indicate that the reaction of the monomers occurs subsequently producing the high molecular weight graft copolymers.

3.2. Micellization behavior of P(HFMA-St-MOTAC)-g-PEG graft copolymer

The critical micelle concentration (CMC) is a measure describing the physical properties of the micelles. When the concentration is above the CMC, the amphiphilic copolymer can self-assemble into an ordered architecture to minimize the interfacial energy. Since the fluorescence spectra of the five samples are similar to each other, only the spectrum of PEG-F60M4.5 at a concentration range

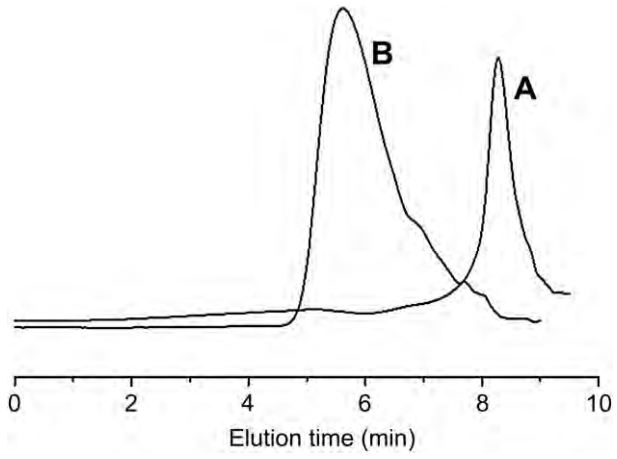

Fig. 4. Typical GPC curves of (A) SPEG, $M_n = 5340$ g/mol and (B) PEG-F60M4.5 (Table 1, Sample 4), $M_n = 1.02 \times 10^5$ g/mol.

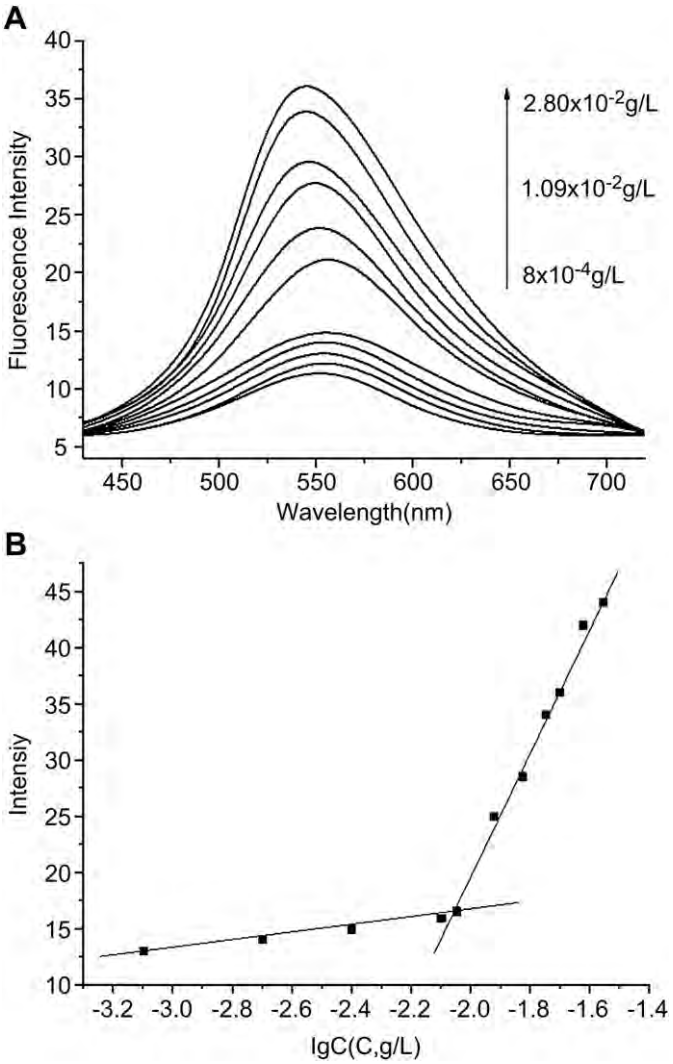

Fig. 5. Fluorescence spectra of PEG-F60M4.5 at different concentrations (The concentrations from bottom to top are 8×10^{-4}, 2×10^{-3}, 4×10^{-3}, 8×10^{-3}, 1×10^{-2}, 1.3×10^{-2}, 1.5×10^{-2}, 1.8×10^{-2}, 2×10^{-2}, 2.4×10^{-2}, 2.8×10^{-2} g/L) (A) and plots of intensity vs. lgC of PEG-F60M4.5 (B). All the measurements are carried out at 25 °C.

from 8×10^{-4} to 2.8×10^{-2} g/L is shown in Fig. 5(A). It can be seen that the emission intensity increases with increasing polymer concentrations. Specifically, at low concentrations, there are small changes in the emission intensity. With increasing concentrations, marked changes in the intensity are observed suggesting a transfer of Nile Red probe to a more hydrophobic microenvironment and indicating formation of micelles. As shown in Fig. 5(B), plots of emission intensity vs. lgC of PEG-F60M4.5 are flat at low concentrations and sigmoidal in the crossover region. The CMC is taken as the intersection of the tangent to the curve at the inflexion with the horizontal tangent through the points at the low polymer concentration. The critical micelle concentrations of the five samples are listed in Table 1. As reported in the literature, the CMC is influenced by many variables, such as the PEG content, temperature, molecular weight, and polydispersity index. The results here indicate that the CMC decreases with increasing HFMA contents in the graft copolymers (PEG-F48M2.1, PEG-F61M2.1, PEG-F67M2.2 in Table 1). This may be due to the unique properties of fluoropolymers such as low surface energy, reduced coefficient of friction, oleo- and hydrophobicity. Therefore, the content of HFMA may become the main factor affecting the CMC value. The experimental results are in good agreement with those previously reported [27].

3.3. In vitro cytotoxicity

Cytotoxicity is an important factor when choosing an appropriate gene delivery vector. The cytotoxicity of PEG-F_XM_Z to CHO cells is evaluated using the MTT assays. Fig. 6 shows the cell viability after 24 h incubation in PEG-F_XM_Z solutions (PEG-F67M2.1, PEG-F61M6.5, PEG-F61M2.1, PEG-F60M4.5 and PEG-F48M2.1) at different concentrations. The results reveal that the cytotoxicity follows a sequence according to the mass, that is, PEG-F61M6.5 > PEG-F60M4.5 > PEG-F61M2.1 > PEG-F67M2.2 > PEG-F48M2.1. The cytotoxicity of PEG-F48M2.1 to CHO cells is the lowest among these groups and the viability remains even when the concentration is up to 1 g/L, while the cytotoxicity of PEG-F61M6.5 is the highest. Exposure of CHO cells to PEG-F61M6.5 micelles produces a dose-dependent reduction in the cell viability. The viability is maintained (>90%) only at a low concentration and when the concentration exceeds 50 μg/mL, the value is reduced. As previously discussed, one of the major drawbacks of cationic polymers non-viral vector is the toxicity effects related to their positive charge. However, in our experiments, the mass percentage content of positively charged MOTAC is low (2.1–6.5%) and consequently, these copolymers have low toxicity.

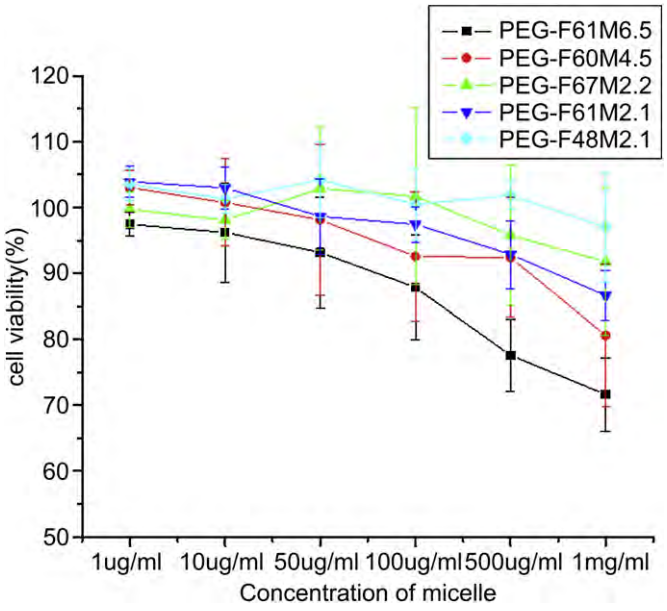

Fig. 6. Cell viability of CHO cells treated with graded doses of micelles for 24 h. Data were the average of at least three independent experiments. Error bars indicate ±SD.

3.4. Fluorescence spectroscopy

The fluorescence spectra of different types of PEG-F_XM_Z in the absence and presence of DNA are shown in Fig. 7 (all the PEG-F_XM_Z concentrations are kept at 0.12 g/L and above CMC). It can be seen from Fig. 7(A) that the pure PEG-F_XM_Z emits three weak peaks at 340, 367, and 470 nm. The fluorescence emission peak at 340 nm is the strongest (from 27.5 to 30.5 for different PEG-F_XM_Z solutions). Upon the addition of DNA, the fluorescence intensity of the PEG-F_XM_Z increases as shown by Fig. 7(B), especially the peak at 340 nm (from 35 to 56.5 for different PEG-F_XM_Z/DNA complexes solutions). When the concentration is above CMC, the PEG-F_XM_Z copolymer can self-assemble into an ordered micelle. This implies that this copolymer micelle can interact with DNA and be protected by DNA efficiently. The interaction between DNA and PEG-F_XM_Z creates

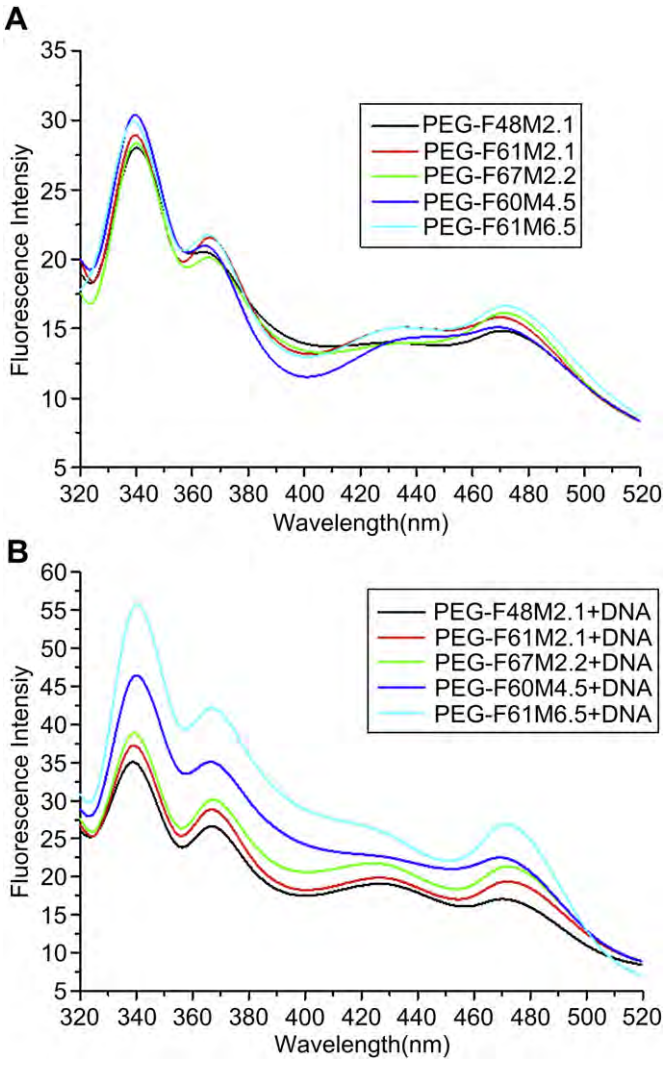

Fig. 7. Fluorescence spectra of (A) PEG-F_XM_Z and (B) PEG-F_XM_Z/DNA complexes (DNA concentration was kept at 90 mg/L, all the PEG-F_XM_Z concentration is kept at 0.12 g/L and volume ratio of PEG-F_XM_Z:DNA is 6:1).

chain entanglement causing changes in the microenvironment around PEG-F_XM_Z. The hydrophobic environment inside the DNA helix reduces the accessibility of solvent water molecules to the PEG-F_XM_Z micelle and the PEG-F_XM_Z mobility is restricted at the binding site, there is decrease in the vibration modes of relaxation followed by increasing fluorescent intensity.

The PEG-F_XM_Z can bind the double stranded DNA by different interactions on the basis of their structure. In the PEG-F_XM_Z aqueous system, there are electrostatic interactions, hydrophobic interactions, and H-bonding, which will influence PEG-F_XM_Z binding to the double stranded DNA. According to Fig. 7(B), when the content of MOTAC in the same and the hydrophobic characteristic contents of HFMA in PEG-F_XM_Z is increased, the fluorescence intensity increases slightly compared to pure PEG-F_XM_Z (PEG-F48M2.1/DNA, PEG-F61M2.1/DNA and PEG-F67M2.2/DNA in Fig. 7(B)). In addition, when the content of HFMA in the PEG-F_XM_Z does not change, increasing the MOTAC contents in the PEG-F_XM_Z leads to marked changes in the intensity as shown by the emission spectra compared to pure PEG-F_XM_Z (PEG-F61M2.1/DNA, PEG-F60M4.5/DNA and PEG-F61M6.5/DNA in Fig. 7(B)). Therefore, the electrostatic interaction [41] between positively charged MOTAC and negatively charged phosphate backbone at the periphery of the double helix DNA are the main factor for PEG-F_XM_Z binding to the double stranded DNA. The hydrophobic interaction due to the hydrophobic characteristic of the fluorinated segments is another factor that PEG-F_XM_Z can bind to the DNA. In addition, as the DNA double helix possesses many hydrogen bonding sites, it is likely that the fluorinated groups of PEG-F_XM_Z forms hydrogen bonds with the DNA consequently increasing the fluorescent intensity. Hence, H-bonding is another reason for the PEG-F_XM_Z binding to the DNA and electrostatic interaction, hydrophobic interaction, and hydrogen bonding exist in this system.

3.5. Viscosity studies

To further explore the interaction characteristics between PEG-F_XM_Z and DNA, the relative specific viscosity of DNA is examined by varying the concentrations of the added PEG-F_XM_Z. Measuring the viscosity of DNA is a classical technique used to analyze the DNA-binding mode in solutions [42]. Hydrodynamic measurements such as viscosity, sedimentation, rotational diffusion, and so on sensitive to molecular lengths provide strong evidence of the DNA-binding modes, especially in the absence of crystallographic structural data [43]. A classical intercalation model demands that the DNA helix lengthens as base-pairs are separated to accommodate the binding molecule, leading to the increase of DNA viscosity. In contrast, a partial, non-classical intercalation of molecule can bend or kink the DNA helix and reduce its effective length and in turn its viscosity [44,45]. When electrostatic binding, groove binding or other outside binding occurs, the viscosity of DNA does not change basically [43,46].

The effects of PEG-F_XM_Z on the viscosity of DNA are shown in Fig. 8. As previously discussed, PEG-F61M6.5 and PEG-F60M4.5 can bind to DNA primarily by the electrostatic mode and it exerts essentially no effect on the DNA viscosity. With increasing amounts of PEG-F48M2.1, PEG-F61M2.1 or PEG-F67M2.2, the relative viscosity of DNA increases steadily. The extent of increase in viscosity ($\Delta\eta$), which may depend on the DNA-binding mode and affinity, follows the order of $\Delta\eta$(PEG-F67M2.2) $>$ $\Delta\eta$(PEG-F61M2.1) $>$ $\Delta\eta$(PEG-F48M2.1). The experimental results suggest that these three graft copolymers can bind DNA via the classical intercalation mode. Owing to the more hydrophobic characteristic of the fluorinated segments, PEG-F67M2.2 can intercalate into the DNA base-pairs more deeply and thus show stronger DNA-binding affinity than PEG-F61M2.1 and PEG-F48M2.1.

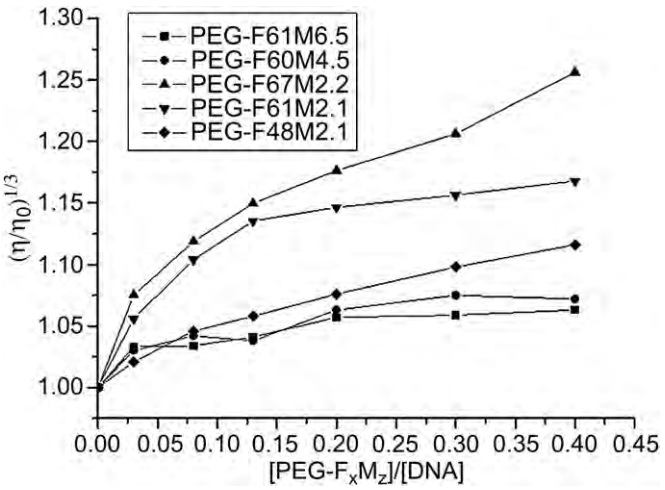

Fig. 8. Effects of increasing the amount of PEG-F_XM_Z on the relative viscosities of DNA at 30.0 ± 0.1 °C. η is the viscosity of DNA in the presence of PEG-F_XM_Z and η_0 is the viscosity of DNA alone. The concentration of DNA is 3 mg/mL.

3.6. Gel electrophoresis of the DNA/copolymer mixture

One prerequisite to polymeric gene carrier is DNA condensation. The condensed form of the copolymer/DNA complexes can protect the plasmid DNA from cell barriers during gene delivery. As shown in Fig. 9, the ability of PEG-F_XM_Z to condense DNA is evaluated using a DNA retardation assay by agarose gel electrophoresis with different types of PEG-F_XM_Z/DNA (Fig. 9(A), weight ratios of PEG-F_XM_Z/DNA is 1.5) and PEG-F60M4.5/DNA (Fig. 9(B) weight ratios of PEG-F60M4.5/DNA ranging from 0 to 1.6:1.). According to Fig. 4(A)

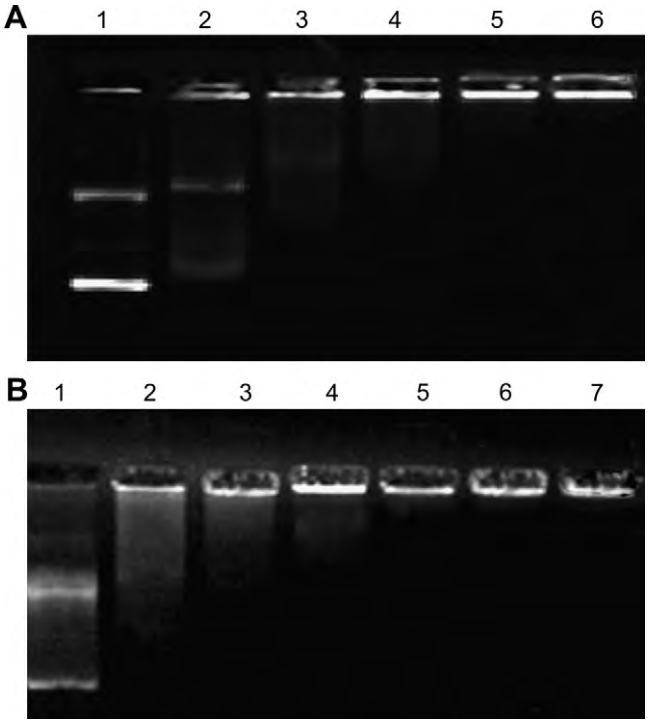

Fig. 9. Agarose gel electrophoresis retardation assay: (A) PEG-F_XM_Z/DNA complexes, Lane 1, naked DNA; lanes 2–6 are PEG-F48M2.1, PEG-F61M2.1, PEG-F67M2.2, PEG-F60M4.5 and PEG-F61M6.5 (weight ratios of PEG-F_XM_Z/DNA is 1.5); (B) PEG-F60M4.5/DNA complexes, Lane 1, naked DNA; lanes 2–7 are PEG-F60M4.5/DNA weight ratios of 0.6–1.6 with increments of 0.2.

Table 3
DNA-binding ability of graft copolymer measure by UV–vis spectrophotometry.

		Volume ratio of PEG-F_XM_Z (H_2O):DNA[a]				
		0.1	0.2	0.4	0.7	1
Absorbency[b]	H_2O/DNA	0.096	0.085	0.072	0.064	0.061
	SPEG-F61D2.1/DNA	/	0.043	0.032	0.022	0.025
	SPEG-F61D2.1/DNA	/	0.032	0.031	0.029	0.028
	SPEG-F67D2.2/DNA	0.035	0.031	0.029	/	/
	SPEG-F60D4.5/DNA	0.031	0.028	0.027	0.021	0.019
	SPEG-F61D6.5/DNA	0.033	0.027	0.025	0.014	/

[a] calf-thymus DNA concentration was kept at 90 mg/L, all the PEG-F_XM_Z concentration was kept at 0.12 g/L and above CMC.
[b] absorption peaks of DNA at 260 nm measure by UV–vis spectrophotometer.

one can see that migration of the plasmid DNA slows when PEG-F_XM_Z is added. However, the PEG-F_XM_Z comprising different MOTAC or HFMA contents shows a different DNA-binding capacity. At a polymer/DNA weight ratio of 1.5, PEG-F60M4.5 and PEG-F61M6.5 can completely retard DNA migration showing a higher DNA-binding capacity than PEG-F67M2.2, PEG-F61M2.1, and PEG-F48M2.1. The results suggest that a high charge density or HFMA content in PEG-F_XM_Z may benefit DNA-binding. As shown in Fig. 9(B), an increase in the PEG-F60M4.5 amount causes a gradual disappearance of the DNA and complete retardation of DNA is achieved at a PEG-F60M4.5/DNA weight ratio of 1:2. These results demonstrate that the copolymers may be used to bind DNA as an efficient gene vector.

3.7. UV–visible spectrophotometry

In addition to gel retardation assay, the DNA-binding ability of the graft copolymers is evaluated by UV–visible spectrophotometry. The PEG-F_XM_Z/DNA complexes are centrifuged and the supernatant is measured at 260 nm which is the absorption peak of DNA. The results are shown in Table 3. Compared to the H_2O/DNA column, after adding PEG-F_XM_Z, the absorbance of the supernatant is significantly reduced. It shows that most of the DNA adsorbs to the PEG-F_XM_Z micelles, and these PEG-F_XM_Z/DNA aggregates are precipitated at the bottom of the complex solutions. It also can be seen from Table 3 that in the SPEG-F60D4.5/DNA and SPEG-F61D6.5/DNA system, the decline in the absorbance value is more than the other three, indicating that SPEG-F60D4.5 and SPEG-F61D6.5 micelles can more easily adsorb DNA compared to the other three. This result is consistent with the gel retardation assay, indicating that high charge density or HFMA contents in PEG-F_XM_Z micelles may benefit DNA-binding. It also shows that the PEG-F_XM_Z micelles which adsorb DNA can be used as an efficient gene vector.

3.8. Characterization of PEG-F_XM_Z/DNA particles

The amphiphilic nature of the PEG-F_XM_Z copolymers provides an opportunity to form micelles in water. Scheme 2 illustrates the assumed structure of the PEG-F_XM_Z copolymer micelles. The micelle has a core–shell structure. The nonionic water-soluble PEG chains serve as a biocompatible outer hydrophilic shell stabilizing the micelles and MOTAC constitutes the positively charged crown. Because of the hydrophobic characteristic of the fluorinated segments, during the self-assembly process, they have a high tendency to bury themselves in the interior of the micelles formed as a hydrophobic core. These tri-layered cationic fluorine-containing amphiphilic graft copolymer micelles are capable for efficient DNA delivery (Scheme 2).

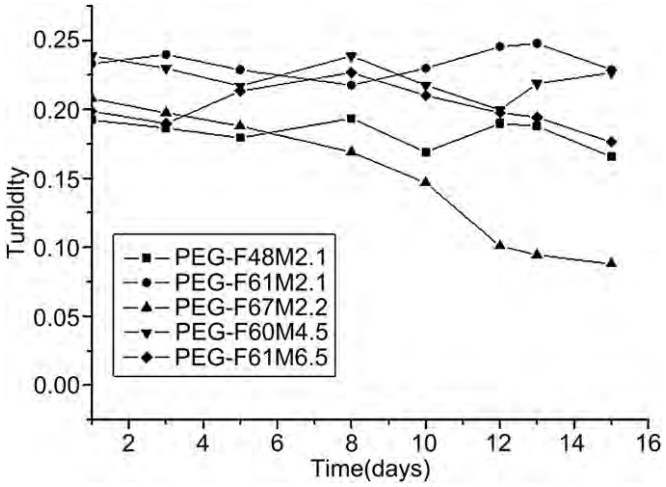

Fig. 10. Dispersive stability of various PEG-F_XM_Z micelles.

All methods reported for amphiphilic copolymers micelles preparation are in general also valid for self-assembled vesicular structures of amphiphilic polymers. The preparation methods can be divided into two groups: solvent free techniques and techniques with the aid of organic solvents. In the first group, the amphiphilic copolymer is in contact with the aqueous medium in its dry state and is subsequently hydrated to yield micelles. This approach offers the advantage that no organic solvent is present in the system and is mandatory in certain applications. In the second group, the amphiphilic copolymer is first dissolved in an appropriate organic solvent and then mixed with water. The organic phase is subsequently excluded utilizing an appropriate technique. Since it is not possible to completely remove all the solvent, the solvent residues may interfere with many applications and may lead to decrease micelles stability and promote aggregation. In this work, we choose the first method to prepare graft copolymers micelles by dissolving the pure copolymers in distilled water with the graft copolymer solutions having concentrations above CMC.

To be non-viral gene vectors, the micelles should have a good dispersive stability in an aqueous media and not aggregate during storage and transfer process [47]. The dispersive stability of the micelles is analyzed by monitoring the change in turbidity of

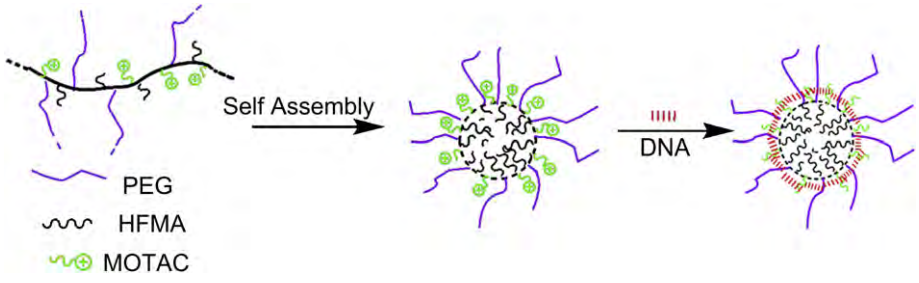

Scheme 2. Schematic drawing of self-assembled of the PEG-F_XM_Z micelle and loading of DNA.

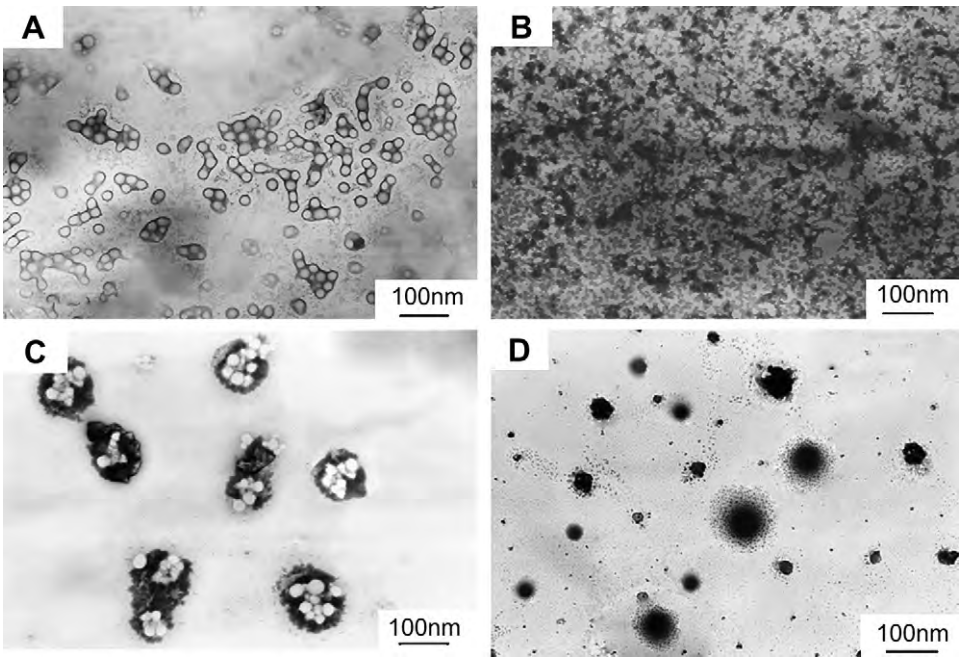

Fig. 11. TEM morphology of PEG-F60M4.5 micelles in aqueous solution (A); pure DNA in aqueous solution (B); PEG-F60M4.5/DNA (volume ratio of PEG-F60M4.5:DNA was 5:1) complexes particles (C), and PEG-F60M4.5/DNA(volume ratio of PEG-F60M4.5:DNA was 1:1) complexes particles (D) (DNA concentration was kept at 90 mg/L, PEG-F60M4.5 concentration was kept at 0.12 g/L).

various PEG-F_XM_Z copolymer micelle solutions (all the PEG-F_XM_Z concentrations are kept at 0.12 g/L and above CMC) as shown in Fig. 10. Owing to the hydrophobic characteristic of the fluorinated segments, they have a high tendency to bury themselves in the interior of the micelles formed as a hydrophobic core. The hydrophobic HFMA core compresses the complexes into smaller and more compact particles, which are very useful for particle stabilization, and the outer hydrophilic PEG chains shell also can stabilize the micelles. As shown in Fig. 10, these cationic fluorine-containing micelles prepared with PEG-F48M2.1, PEG-F61M2.1, PEG-F60M4.5 and PEG-F61M6.5 exhibit no significant change in turbidity even after 15 days of incubation at 37 °C. The hydrodynamic diameter of those micelles also does not change significantly after 15 days (data not shown), indicating excellent dispersive stability. The micelles prepared with PEG-F67M2.2 exhibit a gradual decrease in turbidity 10 days later. On the one hand, the more hydrophobic the segment of HFMA, the higher the hydrophobic force and the copolymer is more prone to secondary or higher level of aggregation. On the other hand, on account of the decrease in the PEG chains, its role in stabilizing the micelles is weakened, resulting in the formation of large micelles during incubation at 37 °C. Hence, the dispersive stability of PEG-F67M2.2 micelles is not good as that of other samples.

Fig. 11(A) exhibits the TEM images of the micelles obtained by self-assembly of the pure PEG-F60M4.5 copolymer with the concentrations of 0.12 g/L in the aqueous solution. The PEG-F60M4.5 copolymer has a good self-assembled morphology manifesting in mainly spherical micelles, the unhydrated micelles diameter are 35 ± 10 nm. The hydrodynamic diameters and size distribution of pure PEG-F60M4.5 micelles in the aqueous medium estimated by PCS are shown in Fig. 12(A). The micelles have a very narrow particle size distribution and the mean diameter of micelles is 60 nm, which is a little larger than that estimated by TEM. This is believed to be due to the presence of water in the PCS experiments inducing swelling of the micelles. There is no significant difference in the morphology among micelles made from the polymers with different PEG-F_XM_Z (same concentration) with the exception of the micelle size in the aqueous medium estimated by PCS increasing

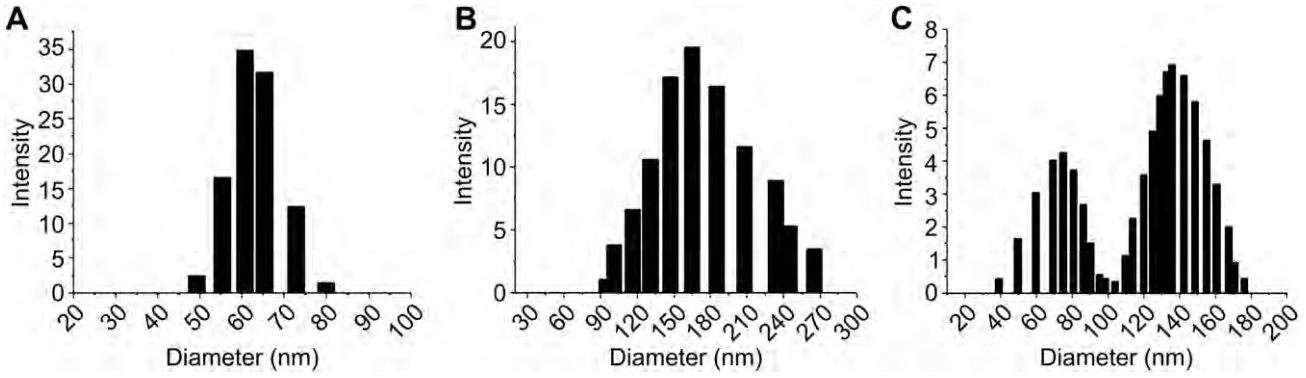

Fig. 12. Hydrodynamic diameters and distribution of pure PEG-F60M4.5 micelles (A); PEG-F60M4.5/DNA (volume ratio of PEG-F60M4.5:DNA is 5:1) complexes particles (B), and PEG-F60M4.5/DNA(volume ratio of PEG-F60M4.5:DNA is 1:1) complexes particles (C). (DNA concentration is kept at 90 mg/L and PEG-F60M4.5 concentration is kept at 0.12 g/L).

Table 4
Zeta potentials of PEG-F60M4.5/DNA complexes with different volume ratios.

Volume ratio (PEG-F60M4.5:DNA)[a]	1:1	2:1	5:1	8:1	10:1	Pure PEG-F60M4.5
Zeta Potential (mV)	-6.99 ± 0.24	3.56 ± 0.17	5.56 ± 0.37	8.56 ± 0.27	11.89 ± 0.5	12.76 ± 0.12

[a] DNA concentration was kept at 90 mg/L, and PEG-F60M4.5 concentration was kept at 0.12 g/L.

slightly (from 50 nm to 95 nm) with increasing fluorine contents in the copolymers. This may be due to more fluorine segments and larger hydrophobic force and the copolymer is more prone to secondary or higher level of aggregation and eventually larger particle size.

Fig. 11(B) displays the TEM images of pure calf-thymus DNA with a concentration of 90 mg/L in the aqueous solution. Pure calf-thymus DNA in the aqueous solution cannot form micelles and do not show clearly in the TEM micrographs. After DNA is added to the PEG-F60M4.5 copolymers solution (volume ratio of PEG-F60M4.5:DNA was 5:1), Fig. 11(C) shows that the morphology, size, and size distribution of the PEG-F60M4.5 micelles change significantly. In comparison with Fig. 11(A), all of the micelles are not scattered. Many micelles (10–20) get together and form large aggregates. In these aggregates, the small micelles are still visible and around those aggregates, there are black adsorbed materials which are DNA by comparing Fig. 11(A) and (B). As previously discussed, because of the formation of the micelle surface with a positive charge and the hydrophobic characteristics of fluorinated segments gathered in the interior of the micelles, they adsorb negatively charge DNA via electrostatic interactions and hydrophobic interactions. However, due to the low DNA concentration, DNA cannot have good coverage on all the surface of the micelles. When water evaporates, the concentration in the solution increases. This leads to an increase in the number density of the micelles and a corresponding decrease in the distance. The DNA adsorbed on the surface of the micelles will increase the absorption capacity to those nearby micelles and then the micelles coalesce together to form large aggregates. The diameter and size distribution of PEG-F60M4.5/DNA (volume ratio is 5:1) complexes particles in the aqueous medium estimated by PCS are shown in Fig. 12(B). PCS measurements demonstrate that the particle size of the PEG-F60M4.5/DNA (volume ratio is 5:1) complexes is much larger than that of pure PEG-F60M4.5 copolymer micelles resulting in large polydispersity.

The morphologies of PEG-F60M4.5/DNA complexes particles when the volume ratio of PEG-F60M4.5:DNA is 1:1 are shown in Fig. 11(D). Comparing Fig. 11(A) and (C), the adsorption phenomenon between PEG-F_XM_Z micelles and DNA is more evident. The majority of the particles are spherical and there is no evidence of the micellar structure such as that shown in Fig. 11(A) and (B). On account of aggregation of the particles which adsorb DNA, some large aggregates (80–100 nm) can be observed in Fig. 11(D). A number of small particles (40–60 nm) can also be observed from Fig. 11(D) and these small particles are formed by a single micelle (Fig. 11(A)) adsorbing the DNA. PCS measurements show typically double peaks (Fig. 12(C)) and have a large polydispersity which is consistent with the TEM results. The large peak shows aggregation of the particles adsorbing DNA.

Further research is carried out to investigate the influence of the HFMA and MOTAC content on the adsorption phenomenon between PEG-F_XM_Z and DNA (volume ratio of PEG-F_XM_Z:DNA is 1:1, DNA concentration is kept at 90 mg/L, and PEG-F_XM_Z concentration is kept at 0.12 g/L). It is found that when the content of MOTAC in the same, with increasing contents of HFMA in PEG-F_XM_Z (PEG-F48M2.1, PEG-F61M2.1 and PEG-F67M2.2), the hydrodynamic diameters of the PEG-F_XM_Z/DNA particles in the aqueous medium estimated by PCS increase slightly (90–150 nm). The morphology of these aggregates does not change significantly (images not shown), except that the PEG-F48M2.1/DNA complex is more uniform than the other two and large aggregates are rare. In addition, when the content of HFMA in PEG-F_XM_Z does not change and the MOTAC contents in PEG-F_XM_Z (PEG-F61M2.1, PEG-F60M4.5 and PEG-F61M6.5) are increased, the diameters of PEG-F_XM_Z/DNA particles in the aqueous medium increase obviously (87–220 nm). The PEG-F61M6.5/DNA aggregates have three peaks ranging from 70 nm to 220 nm. In particular, the TEM photos (image not shown) of the PEG-F61M6.5/DNA complex reveal more and large aggregates, but individual dispersed particles are rare. According to the different TEM and PCS results, it is clear that the electrostatic interactions between positively charged MOTAC and negatively charged DNA are the main factor for the PEG-F_XM_Z micelles adsorbing the calf-thymus DNA resulting in larger particle sizes. The hydrophobic interaction due to the hydrophobic characteristic of the fluorinated segments is another factor for PEG-F_XM_Z micelles adsorbing the calf-thymus DNA. This is also consistent with the fluorescence results.

The surface charge of the vector/gene complexes is very important for gene transfection. Positively charged particles can electrostatically adsorb on the negatively charged cell membrane, and clathrin-dependent endocytosis is responsible for the cellular uptake of the particles [48]. Due to the electrostatic interaction nature between the PEG-F60M4.5 and DNA, both their ratio and environmental conditions should influence the surface charge density of the resultant particles. Therefore, their zeta potentials are measured. As shown in Table 4, the zeta potential of the PEG-F60M4.5/DNA complex increases from -6.99 mV to 11.89 mV with increasing volume ratio. The increase of zeta potential in PEG-F60M4.5/DNA can be understood as the result of the PEG-F60M4.5 micelles adsorbing the DNA.

The stability of the PEG-F_XM_Z/DNA particles is examined by incubating the particles at 37 °C and then measuring the change in the hydrodynamic diameter and zeta potentials of these particles. The particles hydrodynamic diameter and zeta potentials do not change significantly for ~48 h (data not shown) suggesting that the PEG-F_XM_Z/DNA particles have good colloidal stability. The TEM, PCS, and zeta potential results confirm that DNA can readily adsorb onto the PEG-F_XM_Z micelles, and these PEG-F_XM_Z/DNA complex particles have good colloidal stability, suggesting that PEG-F_XM_Z is an excellent matrix for non-viral gene vectors.

4. Conclusion

We have synthesized a series of cationic fluorine-containing amphiphilic graft copolymers P(HFMA-St-MOTAC)-g-PEG comprising poly(hexafluorobutyl methacrylate) (PHFMA), poly-(methacryl oxyethyl trimethylammonium chloride) (PMOTAC), and polystyrene (PSt) backbones, as well as poly(ethylene glycol) (PEG) side chains and evaluated the self-assembly micelle potential from the perspective of a new non-viral gene carrier. The results show that the PEG-F_XM_Z mainly forms spherical micelles in aqueous media (size of 50–95 nm) and stabilization of the hydrophobic HFMA core combined with the PEG antifouling ability can further improve the micelles stability. The critical micelle concentrations of the copolymers measured by fluorescence show that they decrease with increasing HFMA contents in the copolymers. The cytotoxicity

study indicates low cytotoxicity. Fluorescence spectroscopy reveals electrostatic interaction, hydrophobic interaction, and hydrogen bonding in the PEG-F_XM_Z/DNA complexes. Viscosity studies show that the PEG-F61M6.5 and PEG-F60M4.5 can bind DNA primarily via the electrostatic mode whereas PEG-F48M2.1, PEG-F61M2.1 and PEG-F67M2.2 can bind DNA via the classical intercalation mode. The DNA-binding capacity measured by gel retardation assay and UV–vis spectrophotometry discloses that the copolymers have good binding capacity to DNA and suggests that a high charge density or HFMA contents in PEG-F_XM_Z may benefit DNA-binding. TEM, PCS, and zeta potential results show that adsorption occurs readily between PEG-F_XM_Z micelles and DNA and these PEG-F_XM_Z/DNA complex particles have good colloidal stability. These results are important to the application of this non-viral vector in gene delivery system.

Acknowledgments

The work was jointly supported by the Key Projects in the National Science & Technology Pillar Program during the Eleventh Five-year Plan Period (No. 2008BAC32B03) and Hong Kong Research Grants Council (RGG) General Research Funds (GRF) No. CityU 112306.

Appendix

Figures with essential colour discrimination. Figs. 6 and 7 and Scheme 2 in this article may be difficult to interpret in black and white. The full colour images can be found in the on-line version, at doi:10.1016/j.biomaterials.2009.12.014.

References

[1] Olefsky JM. Diabetes-gene therapy for rats and mice. Nature 2000;408:420–1.
[2] Cavazzana-Calvo M, Hacein-Bey S, De Saint Basile G, Gross F, Yvon E, Nusbaum P, et al. Gene therapy of human severe combined immunodeficiency (SCID)-X1 disease. Science 2000;288:669–72.
[3] El-Aneed A. An overview of current delivery systems in cancer gene therapy. J Control Release 2004;94:1–14.
[4] Zhang XJ, Godbey WT. Viral vectors for gene delivery in tissue engineering. Adv Drug Deliv Rev 2006;58:515–34.
[5] Laporte LD, Rea JC, Shea LD. Design of modular non-viral gene therapy vectors. Biomaterials 2006;27:947–54.
[6] Lehrman S. Virus treatment questioned after gene therapy death. Nature 1999;401:517–8.
[7] Bessis N, GarciaCozar FJ, Boissier MC. Immune responses to gene therapy vectors: influence on vector function and effector mechanisms. Gene Ther 2004;11:10–7.
[8] Tian HY, Xiong W, Wei JZ, Wang Y, Chen XS, Jing XB, et al. Gene transfection of hyperbranched PEI grafted by hydrophobic amino acid segment PBLG. Biomaterials 2007;28:2899–907.
[9] Wang CF, Lin YX, Jiang T, He F, Zhuo RX. Polyethylenimine-grafted polycarbonates as biodegradable polycations for gene delivery. Biomaterials 2009;30:4824–32.
[10] Kunath K, Harpe VA, Fischer D, Peterson H, Bickel U, Voigt K, et al. Low-molecular-weight polyethylenimine as a non-viral vector for DNA delivery, comparison of physicochemical properties, transfection efficiency and in vivo distribution with high-molecular-weight polyethylenimine. J Control Release 2003;89:113–25.
[11] Itaka K, Yamauchi K, Harada A, Nakamura K, Kawaguchi H, Kataoka K. Polyion complex micelles from plasmid DNA and poly(ethylene glycol)-poly(L-lysine) block copolymer as serum-tolerable polyplex system: physicochemical properties of micelles relevant to gene transfection efficiency. Biomaterials 2003;24:4495–506.
[12] Cheng H, Zhu JL, Zeng X, Jing Y, Zhang XZ, Zhuo RX. Targeted gene delivery mediated by folate-polyethylenimine-block-poly(ethylene glycol) with receptor selectivity. Bioconjug Chem 2009;20:481–7.
[13] Rekha MR, Sharma CP. Blood compatibility and in vitro transfection studies on cationically modified pullulan for liver cell targeted gene delivery. Biomaterials 2009;30:6655–64.
[14] Mao ZW, Ma L, Yan JA, Yan M, Gao CY, Shen JC. The gene transfection efficiency of thermoresponsive *N,N,N*-trimethyl chitosan chloride-g-poly(*N*-isopropylacrylamide) copolymer. Biomaterials 2007;28:4488–500.
[15] Andersson T, Aseyev V, Tenhu H. Complexation of DNA with poly(methacryl oxyethyl trimethylammonium chloride) and its poly(oxyethylene) grafted analogue. Biomacromolecules 2004;5:1853–61.
[16] Sun TM, Du JZ, Yan LF, Mao HQ, Wang J. Self-assembled biodegradable micellar nanoparticles of amphiphilic and cationic block copolymer for siRNA delivery. Biomaterials 2008;29:4348–55.
[17] Zhu JM, Tang A, Law LP, Feng M, Ho KM, Lee DKL, et al. Amphiphilic core–shell nanoparticles with poly(ethylenimine) shells as potential gene delivery carriers. Bioconjug Chem 2005;16:139–46.
[18] Chaw CS, Chooi KW, Liu XM, Tan CW, Wang L, Yang YY. Thermally responsive core-shell nanoparticles self-assembled from cholesteryl end-capped and grafted polyacrylamides: drug incorporation and in vitro release. Biomaterials 2004;25:4297–308.
[19] Wang CH, Wang CH, Hsiue GH. Polymeric micelles with a pH-responsive structure as intracellular drug carriers. J Control Release 2005;108:140–9.
[20] Choi SW, Yamayoshi A, Hirai M, Yamano T, Takagi M, Sato A, et al. Preparation of cationic comb-type copolymers having high density of PEG graft chains for gene carriers. Macromol Symp 2007;249–250:312–6.
[21] Brus C, Petersen H, Aigner A, Czubayko F, Kissel T. Physicochemical and biological characterization of polyethylenimine-graft-poly(ethylene glycol) block copolymers as a delivery system for oligonucleotides and ribozymes. Bioconjug Chem 2004;15:677–84.
[22] Li LB, Tan YB. Preparation and properties of mixed micelles made of pluronic polymer and PEG-PE. J Colloid Interface Sci 2008;317:326–31.
[23] Pun SH, Bellocq NC, Liu AJ, Jensen G, Machemer T, Quijano E. Cyclodextrin-modified polyethylenimine polymers for gene delivery. Bioconjug Chem 2004;15(4):831–40.
[24] Yang TF, Chen CN, Chen MC, Lai CH, Liang HF, Sung HW. Shell-crosslinked pluronic L121 micelles as a drug delivery vehicle. Biomaterials 2007;28:725–34.
[25] Gao ZG, Fain HD, Rapoport N. Controlled and targeted tumor chemotherapy by micellar-encapsulated drug and ultrasound. J Control Release 2005;102:203–22.
[26] Mao J, Ni PH, Mai YY, Yan DY. Multicompartment micelles from hyperbranched star-block copolymers containing polycations and fluoropolymer segment. Langmuir 2007;23:5127–34.
[27] Hussain H, Busse K, Kressler J. Poly(ethylene oxide)-and poly(perfluorohexylethyl methacrylate)-containing amphiphilic block copolymers: association properties in aqueous solution. Macromol Chem Phys 2003;204:936–46.
[28] Baradie B, Shoichet MS. Novel fluoro-terpolymers for coatings applications. Macromolecules 2005;38:5560–8.
[29] Krafft MP. Fluorocarbons and fluorinated amphiphiles in drug delivery and biomedical research. Adv Drug Deliv Rev 2001;47:209–28.
[30] Riess JG. Blood substitutes and other potential biomedical applications of fluorinated colloids. J Fluor Chem 2002;114:119–26.
[31] Massa TM, McClung WG, Yang ML, Ho JYC, Brash JL, Santerre JP. Fibrinogen adsorption and platelet lysis characterization of fluorinated surface-modified polyetherurethanes. J Biomed Mater Res A 2007;81:178–85.
[32] Ameduri B, Bernard B. Well-architectured fluoropolymers: synthesis, properties and applications. Amsterdam: Elsevier; 2004. pp. 349–54.
[33] Ruiz-Cabello J, Walczak P, Kedziorek DA, Chacko VP, Schmieder AH, Wickline SA, et al. In vivo "hot spot" MR imaging of neural stem cells using fluorinated nanoparticles. Magn Reson Med 2008;60:1506–11.
[34] Lodge TP, Rasdal A, Li ZB, Hillmyer MA. Simultaneous, segregated storage of two agents in a multicompartment micelle. J Am Chem Soc 2005;127:17608–9.
[35] Yang RM, Wang YM, Zhou D. Novel hydroxyethylcellulose-graft-poly acrylamide copolymer for separation of double-stranded DNA fragments by CE. Electrophoresis 2007;28:3223–31.
[36] Liu M, Fu ZS, Wang Q, Xu JT, Fan ZQ. Study of amphiphilic poly(1-dodecene-co-para-methylstyrene)-graft-poly(ethylene glycol): part I. Preparation of poly-(1-dodecene-co-paramethylstyrene) copolymer and its molecular weight regulation. Eur Polym J 2008;44:3239–45.
[37] Chen MQ, Serizawa T, Kishida A, Akashi M. Graft copolymers having hydrophobic backbone and hydrophilic branches. XXIII. Particle size control of poly(ethylene glycol)-coated polystyrene nanoparticles prepared by macromonomer method. J Polym Sci Part A: Polym Chem 1999;37:2155–66.
[38] Manat R, Morten M. POEPOP and POEPS: inert polyethylene glycol crosslinked polymeric supports for solid synthesis. Tetrahedron Lett 1996;37:6185–8.
[39] Gillies ER, Jonsson TB, Frechet JMJ. Stimuli-responsive supramolecular assemblies of linear-dendritic copolymers. J Am Chem Soc 2004;126:11936–43.
[40] Eriksson M, Leijon M, Hiort C, Norden B, Graeslund A. Binding of DELTA- and LAMBDA-$[Ru(phen)_3]2^+$ to [d(CGCGATCGCG)]2 Studied by NMR. Biochemistry 1994;33:5031–40.
[41] Gonzalez-Diaz H, Sanchez-Gonzalez A, Gonzalez-Diaz Y. 3D-QSAR study for DNA cleavage proteins with a potential anti-tumor ATCUN-like motif. J Inorg Biochem 2006;100:1290–7.
[42] Satyanarayana S, Dabrowiak JC, Chaires JB. Neither DELTA- nor LAMBDA-tris(phenanthroline) ruthenium(II) binds to DNA by classical intercalation. Biochemistry 1992;31:9319–24.

[43] Satyanarayana S, Dabrowiak JC, Chaires JB. Tris(phenanthroline)ruthenium(II) enantiomer interactions with DNA: mode and specificity of binding. Biochemistry 1993;32:2573–84.
[44] Brodie CR, Grant Collins J, Aldrich-Wright JR. DNA binding and biological activity of some platinum (II) intercalating compounds containing methyl-substituted 1,10-phenanthrolines. Dalton Trans 2004;8:1145–52.
[45] Allardyce CS, Dyson PJ, Ellis DJ, Heath SL. [Ru(η^6-*p*-cymene)Cl_2(pta)] (pta = 1,3,5-triaza-7-phosphatricyclo-[3.3.1.1]decane): a water soluble compound that exhibits pH dependent DNA binding providing selectivity for diseased cells. Chem Commun 2001;15:1396–7.
[46] Pasternack RF, Gibbs EJ, Villafranca JJ. Interactions of porphyrins with nucleic acids. Biochemistry 1983;22:2406–14.
[47] Maruyama A, Ishihara T, Kim JS, Kim SW, Akaike T. Nanoparticle DNA carrier with poly(L-lysine) grafted polysaccharide copolymer and poly(D, L-lactic acid). Bioconjug Chem 1997;8:735–42.
[48] Petersen H, Fechner PM, Martin AL, Kunath K, Stolnik S, Roberts CJ, et al. Polyethylenimine-graft-poly(ethylene glycol) copolymers: influence of copolymer block structure on DNA complexation and biological activities as gene delivery system. Bioconjug Chem 2002;13:845–54.